Carbon-13 and proton spin relaxation in methane in the gas phase

ARTICLE *in* THE JOURNAL OF PHYSICAL CHEMISTRY · FEBRUARY 1991

Impact Factor: 2.78 · DOI: 10.1021/j100156a015

5 AUTHORS, INCLUDING:

Cynthia J Jameson
University of Illinois at Chicago
205 PUBLICATIONS **4,939** CITATIONS

^{13}C and ^{1}H Spin Relaxation in CH_4 in the Gas Phase

Cynthia J. Jameson,*[1a] A. Keith Jameson,*[1b] Nancy C. Smith,[1a] J. K. Hwang,[1b] and Tasneem Zia[1b]

Departments of Chemistry, University of Illinois at Chicago, Chicago, Illinois 60680, and Loyola University, Chicago, Illinois 60626 *(Received: August 10, 1990)*

The dominance of the spin-rotation mechanism in the relaxation of both the ^{13}C and the ^{1}H nuclear spins in $^{13}CH_4$ in various buffer gases has been established. Cross sections for changes in the rotational angular momentum vector of CH_4 molecules in collisions with various molecules have been obtained as a function of temperature from the measured spin relaxation times of ^{13}C or ^{1}H or both. At 300 K these cross sections are 18.8 ± 0.5 Å^2 (CH_4-CH_4), 16.3 ± 0.3 Å^2 (CH_4-N_2), 15.8 ± 0.2 Å^2 (CH_4-CO), 24 ± 1 Å^2 (CH_4-CO_2), 15 ± 1 Å^2 (CH_4-Ar), 18.3 ± 0.6 Å^2 (CH_4-Kr), 22.4 ± 0.2 Å^2 (CH_4-Xe), 24 ± 1 Å^2 (CH_4-HCl), 25 ± 1 Å^2 (CH_4-CF_4), 34.5 ± 1.1 Å^2 (CH_4-SF_6), and 24.0 ± 0.8 Å^2 (CH_4-SiH_4).

Introduction

CH_4 is of theoretical interest as the simplest spherical top. Studies of the intermolecular potential of CH_4 have largely centered on obtaining the isotropic part of the potential and on the determination of higher electrical moments and polarizabilities by experiment and ab initio calculations. The spectral moments of the collision-induced far-infrared spectrum of CH_4 have been analyzed to give octopole and hexadecapole moments for CH_4.[2a] Spectral moments of collision-induced Raman bands of CH_4 gas yield values for the hyperpolarizabilities A and E.[2b] Ab initio calculations of electric multipole and higher polarizabilities[3] provide the best available values of these electrical properties.

Recent theoretical calculations on the methane pair potential include ab initio SCF calculations fitted to a site-site interaction model[4,5] and calculations of dispersion coefficients.[6] In the calculations of Böhm et al. the parameters of the site-site potential were obtained by applying an uncharged spherical test system (in a rare-gas-like electronic state) for the exponential part and a bare point charge for the $1/R$ part. The remaining contributions are then obtained through a fit to second virial coefficients $B(T)$.[4] Entirely empirical intermolecular potentials have also been proposed in which the isotropic part is obtained by inverting transport and virial coefficients.[7] Addition of a long-range part obtained from collision-induced moments[8] and a short-range anisotropy[9] gives a reasonable fit to the temperature-dependent second virial coefficients. Semiempirical anisotropic potentials determined from solid-state data, virial coefficients, and theoretical long-range dispersion terms[10] come close to reproducing the position of the rainbow oscillation observed in the total differential scattering cross section.[11] The latter data can be fitted well by an analytic semiempirical *spherical* potential;[11] however, none of the potentials, isotropic or anisotropic, give good agreement with all the scattering data and second virial coefficients.[11-13]

CH_4-rare gas anisotropic potentials have been modeled by fitting to diffusion coefficients and thermal diffusion factors,[14] second virial coefficients,[15] mean square torques, and total differential scattering cross sections.[16] A spherical approximation has been used to determine effective isotropic potentials for CH_4-Ne and CH_4-Ar by fitting the parameters to the differential cross sections, viscosity, and second virial coefficients.[17]

Although there exist accurate experimental data in the form of collision-induced spectra and light scattering in gas mixtures containing CH_4,[18,19] from which the pair polarizability anisotropy, higher electrical moments, and polarizabilities may be obtained, there is scarce accurate experimental data to define the short-range interactions. Indeed in CH_4-CH_4 the repulsive parts of the suggested potentials cannot reproduce both the thermal and the high-energy scattering cross section data.[11,12] Recent analysis of all the collision-induced far-infrared spectra of CH_4 over a wide range of temperatures and including the high-frequency region finds that experiment can be brought to agreement only with magnitudes of the ab initio values of the octopole and hexadecapole moments if a short-range anisotropic overlap is included with the octopolar and hexadecapolar induction.[20] Otherwise, unreasonable values of parameters or a strongly temperature-dependent hexadecapole moment would be required to fit the spectra,[21] or else the wings would be significantly underestimated.[22]

In polyatomic molecules the modulation of the intramolecular couplings via reorientation collisions provides the predominant nuclear spin relaxation effects so that it is possible to obtain from spin relaxation times the temperature-dependent cross sections for such collisions. Since spin relaxation is due entirely to the anisotropy of the intermolecular potential, these cross sections provide complementary information to those properties that are primarily dependent on the effective isotropic potential. The cross sections obtained in this study are for CH_4 in collisions with CH_4, Ar, Kr, Xe, N_2, CO, CO_2, HCl, CF_4, SiH_4, and SF_6.

(1) (a) University of Illinois, Chicago. (b) Loyola University.
(2) (a) Birnbaum, G.; Frommhold, L.; Nencini, L.; Sutter, H. *Chem. Phys. Lett.* **1983**, *100*, 292-296. Birnbaum, G.; Cohen, E. R. *J. Chem. Phys.* **1975**, *62*, 3807-3812. (b) Shelton, D. P.; Tabisz, G. C. *Mol. Phys.* **1980**, *40*, 299-308.
(3) Diercksen, G. H. F.; Sadlej, A. *Chem. Phys. Lett.* **1985**, *114*, 187-191. Amos, R. D. *Mol. Phys.* **1979**, *38*, 33-45. John, I. G.; Bacskay, G. B.; Hush, N. S. *Chem. Phys.* **1980**, *51*, 49-60.
(4) Böhm, H. J.; Ahlrichs, R.; Scharf, P.; Schiffer, H. *J. Chem. Phys.* **1984**, *81*, 1389-1395.
(5) Kolos, W.; Ranghini, G.; Clementi, E.; Novaro, O. *Int. J. Quantum Chem.* **1980**, *17*, 429-448.
(6) Fowler, P. W.; Lazzeretti, P.; Zanasi, R. *Mol. Phys.* **1989**, *68*, 853-865. Thomas, G. F.; Mulder, F.; Meath, W. *Chem. Phys.* **1980**, *54*, 45-54.
(7) Matthews, P. G.; Smith, E. B. *Mol. Phys.* **1976**, *32*, 1719-1729.
(8) Isnard, P.; Robert, D.; Galatry, L. *Mol. Phys.* **1976**, *31*, 1789-1811.
(9) Meinander, N.; Tabisz, G. C. *J. Chem. Phys.* **1983**, *79*, 416-421.
(10) Righini, R.; Maki, K.; Klein, M. L. *Chem. Phys. Lett.* **1981**, *80*, 301-305.
(11) Boughton, C. V.; Miller, R. E.; Watts, R. O. *Mol. Phys.* **1985**, *56*, 363-374.
(12) Reid, B. P.; O'Loughlin, M. J.; Sparks, R. K. *J. Chem. Phys.* **1985**, *83*, 5656-5662.
(13) Leonas, V. B.; Sermyagin, A. V. *Chem. Phys.* **1973**, *2*, 462-466. Leonas, V. B. *Sov. Phys. Usp.* **1973**, *15*, 266.
(14) Trengove, R. D.; Robjohns, H. L.; Dunlop, P. J. *Ber. Bunsen-Ges. Phys. Chem.* **1982**, *86*, 951-955.
(15) Brewer, J. *Determination of Mixed Virial Coefficients*; Report No. MRL 2915C AFOSR NO. 67-2795, 1967.
(16) Buck, U.; Schleusner, J.; Malik, D. J.; Secrest, D. *J. Chem. Phys.* **1981**, *74*, 1707-1717.
(17) O'Loughlin, M. J.; Reid, B. P.; Sparks, R. K. *J. Chem. Phys.* **1985**, *83*, 5647-5655.
(18) Thibeau, M.; Berrue, J.; Chave, A.; Dumon, B.; LeDuff, Y.; Gharbi, A.; Oksengorn, B. In *Phenomena Induced by Intermolecular Interactions*; Birnbaum, G., Ed.; Plenum: New York, 1985; pp 291-309. Dagg, I. R. *Ibid.*; pp 95-107.
(19) Meinander, N.; Tabisz, G. C.; Zoppi, M. *J. Chem. Phys.* **1986**, *84*, 3005-3013.
(20) Dore, P.; Moraldi, M.; Poll, J. D.; Birnbaum, G. *Mol. Phys.* **1989**, *66*, 355-373.
(21) Codastefano, P.; Dore, P.; Nencini, L. *J. Quant. Spectrosc. Radiat. Transfer* **1986**, *35*, 255-263.
(22) Dagg, I. R.; Anderson, A.; Yan, S.; Smith, W.; Joslin, C. G.; Read, L. A. A. *Can. J. Phys.* **1986**, *64*, 763-767.

0022-3654/91/2095-1092$02.50/0

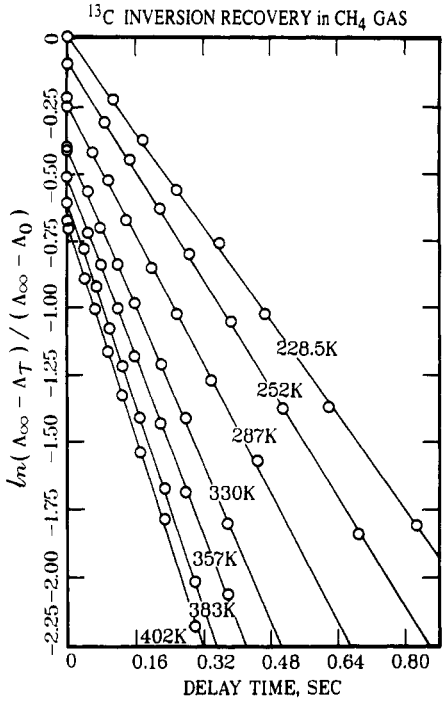

Figure 1. Sample raw data showing results of ^{13}C inversion recovery experiments in pure CH_4 gas, 30.35 amagat. All intercepts are ≈0; the plots have been arbitrarily offset for display of results at different temperatures. The slope of each line is $-1/T_1$.

Experimental Section

Spin relaxation times were measured with the inversion recovery technique using the 5-mm assembly we have described earlier.[23] Sample densities were 5–40 amagat, containing 95 atom % ^{13}C in CH_4 (from Prochem) for the ^{13}C measurements. ^{13}C measurements at 50.28 MHz and ^{1}H measurements at 200 MHz were done on an IBM WP200 Fourier transform NMR spectrometer. The relaxation times in Table I were measured simultaneously (the ^{1}H NMR spectra were obtained with the proton decoupling coil) in order to minimize any differences in experimental conditions that might lead to errors in the ratio $T_1(^1H)/T_1(^{13}C)$. All reported results for ^{13}C measurements in Table II were obtained with gated decoupling. Determination of T_1 from coupled spectra by using the sum of the intensities of the three biggest peaks in the quintets gives results indistinguishable from those determined from spectra obtained with gated decoupling. For example, the measured relaxation time of a 24-amagat sample of pure CH_4 was 0.224 ± 0.001 s (coupled) compared with 0.228 ± 0.003 s (decoupled); for a 16-amagat sample 0.172 ± 0.002 s (coupled) compared with 0.175 ± 0.003 s (decoupled). Continuous broadband decoupling was not used because this leads to systematic errors arising from local heating of the sample during spectrum acquisition. Typical data are shown in Figure 1. The relative error in T_1 is typically less than 1%. The sample temperature was determined with a sealed standard ethylene glycol or methanol sample prior to each run. This is a necessary calibration for each temperature because the temperature read by the thermocouple beneath the sample is that of the heat-exchange gas flowing into the sample chamber and is not necessarily the same as that in the sample itself. The difference between the temperature indicated and the actual temperature of the sample can be substantial, depending on the location of the thermocouple. The problem becomes exaggerated as the set value differs greatly from ambient temperature.

It is particularly important to scrupulously exclude oxygen from samples for ^{1}H T_1 measurements, even in the gas phase. The generally small paramagnetic shielding for protons in molecules translates to a small factor for spin rotation relaxation rates. For ^{1}H in CH_4 the intermolecular nuclear spin–electron spin dipolar mechanism due to small amounts of O_2 becomes competitive with the spin–rotation mechanism at 0.5% O_2.[24] We removed trace amounts of O_2 that may have been contaminants in the buffer gases by using a small amount of SiH_4 in each sample. SiH_4 spontaneously reacts with O_2, yielding trace amounts of diamagnetic products causing no noticeable errors. A sample contained, typically, 1 amagat each of CH_4 and SiH_4 and 10–40 amagat of buffer gas. A minor correction, $(T_1/\rho)_{CH_4\text{-}SiH_4}\rho_{SiH_4}$ was made in each measured T_1.

Domination of the Spin Rotation Mechanism in CH_4 in the Gas Phase

In a spherical top the spin rotation relaxation time in the extreme narrowing limit (which holds for all the densities used in this study) is given by[25]

$$T_1 = \frac{3}{2\langle J(J+1)\rangle C_{eff}^2}\frac{1}{\tau_{SR}} = \frac{\hbar^2}{2C_{eff}^2 I_0 kT}\frac{1}{\tau_{SR}} \quad (1)$$

where

$$C_{eff}^2 = C_{av}^2 + {}^4/_{45}(\Delta C)^2 \quad (2)$$

Centrifugal distortion partially removes the degeneracy of the states characterized by the J quantum number when the permutation symmetry of the four protons in CH_4 is taken into account.[26] It has been shown that the ΔC term connects states whose energies differ by the centrifugal distortion energy. Thus, in the derivation of T_1 the effect of centrifugal distortion needs to be taken into account because in CH_4 these states are separated by an amount (200 MHz) very close to the Larmor frequency. However, it has been shown that this effect is not observable for ^{1}H for densities >0.5 amagat.[27] Since $\Delta C = 0$ for ^{13}C in CH_4, only the C_{av} term contributes to $T_1(^{13}C)$ anyway, and centrifugal distortion effects cannot influence $T_1(^{13}C)$. Therefore, in the density regime of our experiments, both ^{13}C and ^{1}H relaxation in CH_4 can be interpreted without considering centrifugal distortion, that is, we may use eqs 1 and 2 in interpreting our observed T_1 values.

The spin–rotation constants for CH_4 are $C_{av} = {}^1/_3(2C_\perp + C_\parallel) = 10.4 \pm 0.1$ kHz, $\Delta C = C_\parallel - C_\perp = 18.5 \pm 0.5$ kHz for ^{1}H, and $C_{av} = 15.94 \pm 2.37$ kHz for ^{13}C from molecular beam measurements in the ground vibrational state.[28] A thermal average value of C_{av} can also be obtained from the known relationship between the spin–rotation constant and the paramagnetic shielding,[29] the theoretically calculated diamagnetic shielding, and the absolute shielding of ^{1}H and ^{13}C in CH_4 gas in the zero-pressure limit.[30] The ^{13}C chemical shift in $^{13}CH_4$ relative to ^{13}CO in the zero-pressure limit and the ^{13}CO absolute shielding give $\sigma_0(^{13}C \text{ in } CH_4) = 195.1$ ppm,[31] from which we calculate

$$\sigma^{SR} = \sigma_0 - \sigma^d + \frac{e^2}{3mc^2}\sum_i Z_i/r_i = -67.06 \text{ ppm}$$

using $\sigma^d = 296.5$ ppm.[32] We may then calculate C from the well-known relationship between the shielding and the spin–rotation constant

(23) Jameson, C. J.; Jameson, A. K.; Buchi, K. *J. Chem. Phys.* **1986**, *85*, 697–700. Jameson, C. J.; Jameson, A. K.; Smith, N. C. *J. Chem. Phys.* **1987**, *86*, 2717–2722.

(24) Jameson, C. J.; Jameson, A. K.; Hwang, J. K. *J. Phys. Chem.* **1989**, *93*, 634–638.

(25) Gordon, R. G. *J. Chem. Phys.* **1966**, *44*, 228–234.

(26) Hecht, K. T. *J. Mol. Spectrosc.* **1960**, *5*, 355, 390.

(27) (a) Beckmann, P. A.; Bloom, M.; Burnell, E. E. *Can. J. Phys.* **1972**, *50*, 251–258. (b) Beckman, P. A.; Bloom, M.; Ozier, I. *Can. J. Phys.* **1976**, *54*, 1712–1727.

(28) Yi, P. N.; Ozier, I.; Ramsey, N. F. *J. Chem. Phys.* **1971**, *55*, 5215–5227; Ozier, I.; Vitkevich, J. A.; Ramsey, N. F. *Abstr., 27th Symp. Mol. Spectrosc.* **1972**.

(29) Flygare, W. H. *J. Chem. Phys.* **1964**, *41*, 793–800.

(30) Raynes, W. T. *Nuclear Magnetic Resonance*; Royal Society of Chemistry: London, 1978; Vol. 7, pp 1–25.

(31) Jameson, A. K.; Jameson, C. J. *Chem. Phys. Lett.* **1987**, *134*, 461–466.

(32) Höller, R.; Lischka, H. *Mol. Phys.* **1980**, *41*, 1017–1040.

$$C = 2(m/m_p)B_0 g(^{13}C)\sigma^{SR} = -16.121 \pm 0.24 \text{ kHz}$$

assuming σ^{SR} is known to ±1 ppm. This is in good agreement with the molecular beam data, $C = -15.94 \pm 2.37$ kHz,[28] and is more precise. We therefore use $C = -16.121 \pm 0.24$ kHz from the chemical shift scale. A similar comparison can be made of the ^1H chemical shift and $C_{av}(^1H)$ from molecular beam spectroscopy. In this case the quoted error estimate in the experimental value of C_{av} translates to ±0.1 ppm in chemical shift. Once again we use the relationship

$$\sigma^{SR} = \frac{C_{av}}{B_0}\frac{m_p}{2mg(^1H)}$$

and from $C_{av} = 10.4 \pm 0.1$ kHz we calculate $\sigma^{SR}(^1H) = 10.88 \pm 0.1$ ppm so that

$$\sigma_0 - \sigma^d = \sigma^p = \sigma^{SR} - \frac{e^2}{3mc^2}\sum_i Z_i/r_i = -56.4 \pm 0.1 \text{ ppm}$$

The "best" quoted value for $\sigma_0(^1H$ in $CH_4)$ is 30.611 ppm[30] in the ^1H shielding scale, so that the "experimental" σ^d derived from C_{av} is 87.0 ± 0.1 ppm. This is in excellent agreement with theoretical ab initio calculations, which give $\sigma^d = 87.9$ ppm.[31]

The rotational constant for $^{13}CH_4$ is 5.240 82 cm^{-1}.[33] The use of $^3/_2(kT/B_0)$ for $\langle J(J+1)\rangle$ in eq 1 is in error by less than 1% at 200 K and is an even better approximation at 400 K.

The dominance of the spin rotation mechanism in CH_4 can be established. The other mechanisms in CH_4 give relaxation rates that are orders of magnitude smaller than spin–rotation. Estimates of these rates can be made if we assume that the correlation times in the gas phase are about the same for all mechanisms and related to $(\rho\bar{v}\sigma)^{-1}$. It is expected from Gordon's theory that the cross section σ_θ for dipole-dipole relaxation has a different dependence on the anisotropy of the inter-molecular potential than σ_J for spin–rotation relaxation. However, for purpose of estimating the competing mechanisms, let us assume the cross sections are the same for all of them. Then the molecular factors that determine the magnitudes of the fluctuating local magnetic fields can be used to estimate ratios of relaxation rates.

The chemical shift anisotropy and intermolecular nuclear dipole–dipole mechanisms can be ruled out immediately. In the gas phase these relaxation rates involve factors $^2/_{15}(\omega\Delta\sigma)^2$ and $8\gamma^4\hbar^2I(I+1)\pi\rho^2$ (or $4\gamma_I{}^2\gamma_S{}^2\hbar^2\pi\rho^2$), respectively.[34] The ratios of these factors to the factor $C_{eff}{}^2kT/B_0$ in the spin–rotation mechanism are respectively $(1/T_1)_{CSA}/(1/T_1)_{SR}$ and $(1/T_1)_{DD}/(1/T_1)_{SR}$. These ratios are 0 and 9×10^{-8} for ^{13}C and 1.0×10^{-4} and 5×10^{-6} for ^1H in a 10-amagat CH_4 sample. CH_4 is a good candidate for a possible contribution of intramolecular dipole–dipole (DD) interactions to the relaxation time since the CH bond distance is short (1.0940 Å).[32] The ratio of the factor $\gamma_I{}^2\gamma_S{}^2\hbar^2/r_{CH}{}^6$ to $C_{eff}{}^2kT/B_0$ is 1.3×10^{-2} for ^{13}C and 3×10^{-2} for ^1H at 300 K. In the gas the correlation times for SR and DD differ by a factor of 2.9, so the two relaxation mechanisms could be competitive at low temperatures. However, it can be shown that this mechanism is also unimportant at the temperatures of our studies.

There are several ways of experimentally verifying the domination of the spin–rotation mechanism in the relaxation of ^{13}C and ^1H in CH_4 in the gas phase: (1) If relaxation is entirely by spin–rotation, then the ratio $T_1(^1H)/T_1(^{13}C)$ should be independent of density and temperature and magnetic field and should be equal to $C_{eff}{}^2(^{13}C)/C_{eff}{}^2(^1H)$ obtained from independent experiments. (2) The temperature dependence of T_1/ρ for the spin–rotation mechanism is $T^{-3/2}$ or close to it, whereas the intramolecular dipole–dipole mechanism gives $T_1 \sim T^{-1/2}$. (3) There should be no observable nuclear Overhauser enhancement (NOE). NOE arises in spin I when there are cross relaxation effects between two unlike spins I and S, such as dipole–dipole interactions that are time dependent due to rapid relaxation of spin S, usually proton.[35] An NOE effect can be observed as the difference between spectra obtained with the continuous-wave proton decoupler on-resonance and off-resonance during the preparation period. The NOE is defined as the fractional enhancement of the integrated intensity of the ^{13}C when the ^1H is saturated compared to that of the normal spectrum. We verified (vide infra) that the spin–rotation mechanism is dominant for both ^{13}C and ^1H in CH_4 in the gas phase by all three criteria.

TABLE I: Comparison of ^1H and ^{13}C Relaxation Times in the Same Sample of 36.6-amagat Pure CH_4

T/K	$T_1(^1H)$/s	$T_1(^{13}C)$/s	$T_1(^1H)/T_1(^{13}C)$
220	1.090 ± 0.005	0.565 ± 0.005	1.93 ± 0.03
260	0.861 ± 0.007	0.460 ± 0.002	1.87 ± 0.02
300	0.735 ± 0.006	0.379 ± 0.006	1.94 ± 0.05
360	0.600 ± 0.005	0.321 ± 0.005	1.87 ± 0.04

TABLE II: Characteristic Spin Relaxation Parameters for ^{13}C in CH_4 Due to Interaction with Various Other Molecules

	T/K	(T_1/ρ)/ms amagat^{-1}
CH_4–CH_4	230–400	$(10.2 \pm 0.5)(T/300)^{-1.43\pm0.02}$
CH_4–Ar	220–400	$(7.2 \pm 0.4)(T/300)^{-1.59\pm0.08}$
CH_4–HCl	250–400	$(11.6 \pm 0.5)(T/300)^{-1.53\pm0.08}$
CH_4–CO_2	255–400	$(10.8 \pm 0.2)(T/300)^{-1.60\pm0.06}$
CH_4–CF_4	220–400	$(11.9 \pm 0.5)(T/300)^{-1.59\pm0.06}$

The ratio of the ^1H relaxation time to the ^{13}C relaxation time measured in the same sample at the same temperature is constant within experimental errors, $T_1(^1H)/T_1(^{13}C) = 1.90 \pm 0.05$. Some typical numbers are shown in Table I. With the ^{13}C and ^1H spin–rotation constants from molecular beam data,[28] the ratio $C_{eff}{}^2(^{13}C)/C_{eff}{}^2(^1H) = 1.83 \pm 0.11$. On the other hand, with $C(^{13}C) = 16.12 \pm 0.1$ kHz from the ^{13}C absolute shielding scale, the ratio $C_{eff}{}^2(^{13}C)/C_{eff}{}^2(^1H) = 1.87 \pm 0.07$. Both agree well with the observed ratio of relaxation times, 1.90 ± 0.05, which indicates that the spin–rotation relaxation mechanism is dominant in CH_4 in the gas phase.

A further check is provided by the NOE experiment. The difference spectrum should reveal any increase in ^{13}C signal intensity when the protons are saturated. We find no enhancement at all, i.e., the difference spectrum provides an upper limit of 0.02 to the ratio $(1/T_1)_{DD}/(1/T_1)_{SR}$ at room temperature, substantiating our estimate that the DD rate is nearly 2 orders of magnitude smaller than the SR rate. Therefore, the intramolecular dipolar contributions to the ^{13}C and ^1H relaxation in CH_4 in the gas phase are insignificant. This is in sharp contrast to ^1H in liquid CH_4, for example, in which it has been reported that $(1/T_1)_{SR} = 3.54 \times 10^{-2}$ s^{-1} and $(1/T_1)_{DD} = 2.08 \times 10^{-2}$ s^{-1} at 174 K.[36] The relaxation time associated with SR in the liquid (28.3 s) is much longer than 0.2 s for ^1H T_{1SR} in a 10-amagat sample in our study.

Having established that both ^{13}C and ^1H relaxation in CH_4 in the gas phase are dominated by the spin–rotation mechanism, we then only need to measure *either* ^{13}C or ^1H relaxation times in samples of various densities of CH_4 and buffer gas as a function of temperature. The additivity of spin–rotation relaxation times allows us to determine (T_1/ρ) for CH_4–buffer collisions from

$$T_1 = (T_1/\rho)_{CH_4\text{–}CH_4}\rho_{CH_4} + (T_1/\rho)_{CH_4\text{–buffer}}\rho_{buffer}$$

Results are shown in Tables II and III. Figures 2 and 3 show that the observed temperature dependence for each CH_4–buffer pair can be expressed by

$$(T_1/\rho) = (T_1/\rho)_{300\,K}(T/300)^n$$

where n is close to $-^3/_2$, the signature of the spin–rotation mechanism.[37] The intramolecular dipolar mechanism, on the

(33) Bendtsen, J. *J. Raman Spectrosc.* **1974**, *2*, 133. Pinkley, L. W.; Rao, K. N.; Nhu, M. D.; Tagarro, G.; Poussigne, G. *J. Mol. Spectrosc.* **1976**, *63*, 402–444.

(34) Abragam, A. *The Principles of Nuclear Magnetism*; Clarendon Press: Oxford, 1961.

(35) Noggle, J. H.; Schirmer, R. E. *The Nuclear Overhauser Effect*; Academic Press: New York, 1971.

(36) Oosting, P. H.; Trappeniers, N. J. *Physica* **1971**, *51*, 395–417.

(37) Johnson, C. S.; Waugh, J. S. *J. Chem. Phys.* **1961**, *35*, 2020.

TABLE III: Spin Relaxation Times for ^1H in CH_4 Due to Interaction with Other Molecules

	this work		lit. values		
	(T_1/ρ)/ms amagat^{-1}	T/K	(T_1/ρ)/ms amagat^{-1}	T/K	ref
CH_4-CH_4	$(20.2 \pm 0.4)(T/300)^{-1.40\pm0.03}$	230–400	$20.5(T/300)^{-1.5}$	100–700	*a*
CH_4-Ar	$(13.3 \pm 0.5)(T/300)^{-1.29\pm0.05}$	225–400	$(14.3 \pm 0.9)(T/300)^{-1.25\pm0.09}$	300–600	38
CH_4-Kr	$(15.6 \pm 0.5)(T/300)^{-1.37\pm0.04}$	230–400			
CH_4-Xe	$(18.4 \pm 0.1)(T/300)^{-1.56\pm0.02}$	250–400			
CH_4-N_2	$(15.9 \pm 0.3)(T/300)^{-1.37\pm0.03}$	230–400	$(13.94 \pm 1.21)(T/300)^{-0.87\pm0.14}$	300–600	38
CH_4-CO	$(15.4 \pm 0.2)(T/300)^{-1.33\pm0.02}$	230–400			
CH_4-HCl	$(22.0 \pm 0.4)(T/300)^{-1.40\pm0.06}$	290–400			
CH_4-CO_2	$(21.9 \pm 1.0)(T/300)^{-1.48\pm0.10}$	280–400	$(21.97 \pm 1.35)(T/300)^{-0.91\pm0.10}$	300–600	38
CH_4-CF_4	$(20.7 \pm 0.6)(T/300)^{-1.30\pm0.04}$	255–400			
CH_4-SiH_4	$(22.8 \pm 0.8)(T/300)^{-1.61\pm0.04}$	225–400			
CH_4-SF_6	$(28.2 \pm 0.9)(T/300)^{-1.32\pm0.08}$	290–400			

[a] Data in ref 27b corresponds to $20.5(T/300)^{-1.38}$ for T = 110–295 K. Earlier reports were 21.9 ± 0.4 at 295 K (ref 27a) and $21.8(T/300)^{-1.47\pm0.03}$ for T = 300–600 K (ref 38). For 100–700 K, data from refs 39 and 40 fit $T^{-1.50}$.

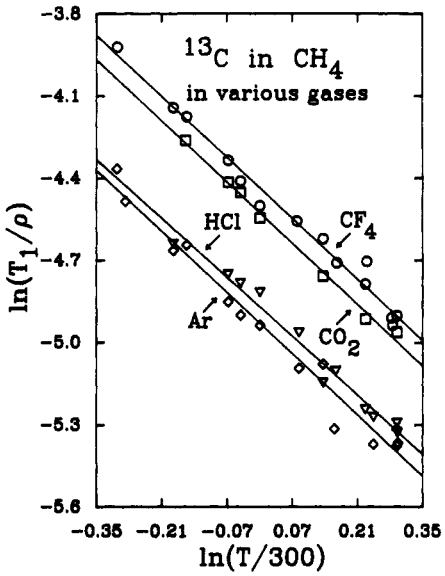

Figure 2. Temperature dependences of (T_1/ρ) for ^{13}C in CH_4 in various buffer gases are all very close to $T^{-3/2}$.

other hand, has an expected T dependence $\sim T^{-1/2}$. This is further confirmation that the dominant relaxation mechanism is spin rotation. The (T_1/ρ) values for ^1H in pure $^{13}CH_4$ compared to that in pure $^{12}CH_4$ are in the ratio 20.2/19.6 = 1.03, which is fortuitously exactly that expected from the mass factors in $\tilde{v}$, i.e., $[m(^{13}CH_4)/m(^{12}CH_4)]^{1/2}$.

Cross Sections for Angular Momentum Transfer

The fortunate dominance of the SR mechanism in the gas phase allows us to directly obtain cross sections for rotational angular momentum transfer from our T_1 data. In the extreme narrowing limit, the T_1 values are directly related to cross sections by $\tau_{SR} = (\rho\tilde{v}\sigma_J)^{-1}$:[25]

$$(T_1/\rho) = \frac{\tilde{v}}{2C_{eff}^2\langle J(J+1)\rangle}\sigma_J(T) \qquad (3)$$

Thus, each experimental point in the plots shown in Figures 2 and 3 gives a cross section $\sigma_J(T)$ for CH_4 with a collision partner. Cross sections obtained from our ^1H relaxation data are in complete agreement with cross sections obtained from our ^{13}C data where both have been measured. These are shown in Table IV. If the value of the ^{13}C spin–rotation constant is perfectly consistent with the values of the ^1H spin–rotation constants, then the cross sections from the ^{13}C T_1 measurements and those from the ^1H T_1 measurements in the same sample should be identical within the errors of the T_1 measurements. We see in Table IV that the cross sections derived from the ^{13}C and ^1H measurements in the $^{13}CH_4$–X and $^{12}CH_4$–X samples are within 5% of each other. Note that the $C_{eff}^2(^{13}C)$ obtained from the T_1 ratio in pure CH_4 and that value we used to calculate the cross section differ by a factor 1.013; apparent systematic differences of at least this magnitude in the two cross sections can thus be expected. In principle, there should be an intrinsic slight difference in cross section for $^{12}CH_4$–X compared to $^{13}CH_4$–X, due to a dependence of σ_J on the reduced mass of the collision pair. This has not been explored, is not evident here, and in any case is probably a small difference entirely within the error bars quoted here. We conclude that our T_1 data and the resulting cross sections are all consistent, independent of the probe nucleus used. Such consistency is possible because the spin–rotation relaxation mechanism completely dominates both ^{13}C and ^1H spin relaxation in the gas phase at these temperatures.

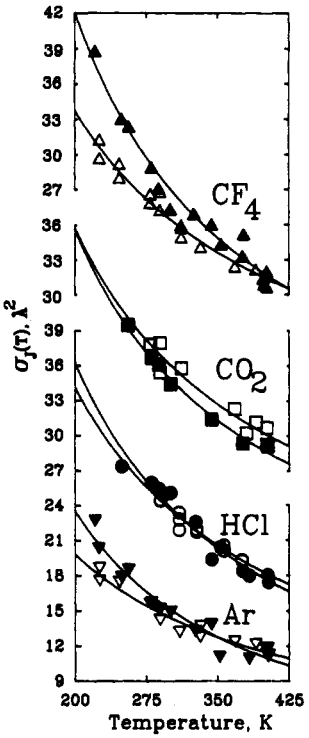

Figure 3. Cross sections for rotational angular momentum transfer σ_J for the CH_4 molecule with various collision partners, obtained independently from ^{13}C (filled symbols) and from ^1H (open symbols) T_1 in CH_4–CF_4, CH_4–CO_2, CH_4–HCl, and CH_4–Ar gas mixtures containing $^{13}CH_4$ and $^{12}CH_4$, respectively. The curves are the least-squares fit to a power law, $\sigma_J(T) = \sigma_J(300\text{ K})(T/300)^m$, where $\sigma_J(300\text{ K})$ and m are the values shown in Table IV.

All cross sections decrease with increasing temperature as shown in Figure 4. These curves are reasonably well represented by a function of the form

$$\sigma_J(T) = \sigma_J(300\text{ K})(T/300)^m \qquad (4)$$

(38) Rajan, S.; Lalita, K.; Babu, S. V. *J. Magn. Reson.* **1974**, *16*, 115–129; *Can. J. Phys.* **1975**, *53*, 1624–1630, 1631–1634.
(39) Lalita, K.; Bloom, M. *Chem. Phys. Lett.* **1971**, *8*, 285–287.
(40) Bloom, M.; Bridges, F.; Hardy, W. N. *Can. J. Phys.* **1967**, *45*, 3533.

TABLE IV: Cross Sections for Rotational Angular Momentum Transfer for CH_4 Molecule with Various Collision Partners,[a] $\sigma_J(T)$, Å²

pair	from ^{13}C T_1	from ^1H T_1[c]	from lit.	ref
CH_4–CH_4	$(19.2 \pm 0.2)(T/300)^{-0.93\pm0.02}$	$(18.4 \pm 0.4)(T/300)^{-0.90\pm0.03}$	$18.5(T/300)^{-1.0}$[b]	27b, 39, 40
CH_4–Ar	$(15.1 \pm 0.9)(T/300)^{-1.09\pm0.08}$	$(14.4 \pm 0.5)(T/300)^{-0.79\pm0.05}$	$(15.5 \pm 1.0)(T/300)^{-0.75\pm0.09}$	38
CH_4–Kr		$(18.3 \pm 0.6)(T/300)^{-0.87\pm0.04}$		
CH_4–Xe		$(22.4 \pm 0.2)(T/300)^{-1.06\pm0.02}$		
CH_4–N_2		$(16.3 \pm 0.3)(T/300)^{-0.87\pm0.03}$	$(14.3 \pm 1.3)(T/300)^{-0.37\pm0.14}$	38
CH_4–CO		$(15.8 \pm 0.2)(T/300)^{-0.83\pm0.02}$		
CH_4–HCl	$(23.9 \pm 0.9)(T/300)^{-1.03\pm0.08}$	$(23.7 \pm 0.4)(T/300)^{-0.90\pm0.06}$		
CH_4–CO_2	$(22.9 \pm 0.5)(T/300)^{-1.10\pm0.06}$	$(24.1 \pm 1.0)(T/300)^{-0.98\pm0.10}$	$(24.2 \pm 1.5)(T/300)^{-0.41\pm0.10}$	38
CH_4–CF_4	$(27.0 \pm 1.1)(T/300)^{-1.09\pm0.06}$	$(24.4 \pm 0.7)(T/300)^{-0.80\pm0.04}$		
CH_4–SiH_4		$(24.0 \pm 0.8)(T/300)^{-1.11\pm0.04}$		
CH_4–SF_6		$(34.5 \pm 1.1)(T/300)^{-0.82\pm0.08}$		

[a] Temperature ranges are the same as in Tables II and III. Calculated by using spin–rotation constants from ref 28 for ^1H in $^{12}CH_4$ and −16.121 kHz for ^{13}C in $^{13}CH_4$ (see text). Quoted errors are standard deviations. [b] For T = 100–700 K. Reference 27b gives $18.5(T/300)^{-0.88}$. [c] Room-temperature cross sections obtained from ^1H T_1 for $^{13}CH_4$–X are comparable with those shown above for $^{12}CH_4$–X.

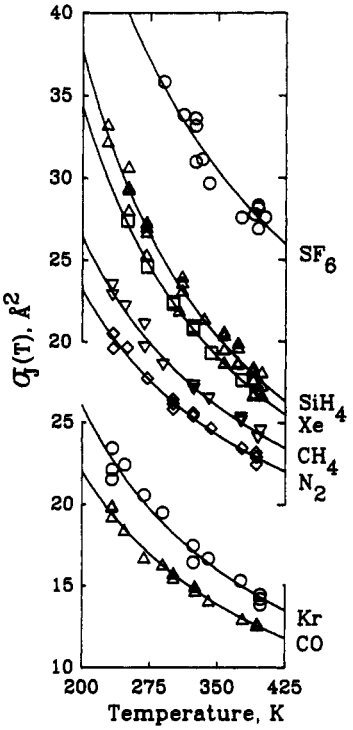

Figure 4. Cross sections for rotational angular momentum transfer σ_J for CH_4 molecule in CH_4–X collisions, obtained from ^1H T_1 in $^{12}CH_4$ molecule in various gases. The curves are the least-squares fit to a power law $\sigma_J(T) = \sigma_J(300\text{ K})(T/300)^m$, where $\sigma_J(300\text{ K})$ and m are the values shown in Table IV.

where m is close to −1. This temperature dependence is to be expected from the classical interpretation of $\sigma_J(T)$, which is[25]

$$\sigma_J(T) = (1/\langle J^2\rangle^T)\int_0^\infty (\mathbf{J}_f - \mathbf{J}_i)^2 2\pi b\, db$$

In Gordon's semiclassical theory,[41] $\sigma_J(T)$ is a thermal average cross section obtained from sigma matrix elements for specific J and m_J changes, weighted by $\sim J^2$ times the population of the initial J level. Various types of collisions contribute to the sigma matrix, depending on the anisotropy of the potential. At the lower relative velocities at lower temperatures the attractive field is more important. Both reorientation and inelastic processes that contribute to the cross section are more efficient at low J values, which are more populated at lower temperatures. Trajectory calculations on other systems such as HCl–Ar verify this qualitative general behavior.[41] Indeed, $\sigma_J(T)$ decreases with increasing temperature in all other systems that we have studied.

(41) Neilsen, W. B.; Gordon, R. G. *J. Chem. Phys.* **1973**, *58*, 4131–4148, 4149–4170.

TABLE V: Comparison of Various Types of Cross Sections, Å², for CH_4–CH_4 at Room Temperature

type	value, Å²	ref
σ_{geom}	43.5[a]	43
$\sigma(02\pi)$	33 ± 2[b]	44
$\sigma(12q)$	57[a]	45
$\sigma'(0\hat{2})$ or σ_θ	53[d]	46, 47
$\sigma'(0\hat{1})$ or σ_j	18 (this work)	
$\sigma(0001)$	5.4,[e] 5.3[f]	48, 49
$\sigma_{rot}(0001)$	6.5[g]	50
$\sigma(1001)$	34.04[i]	48
$\sigma(1010)$	32.71[i]	48
$\sigma(20)$	41.15,[i] 42.4 ± 0.4[h]	48, 51
$\sigma(10E)$	29.54[i]	48
$\sigma(10D)$	37.00[i]	48
σ_{rot}(IRDR)	41.9 ± 0.8[g]	52
σ_{PB}(IR)	69[g]	54
σ_{PB}(Raman, Q)	82[g]	55

[a] $\sigma_{geom} = \pi r_0^2$, where r_0 is 3.7205 Å from ref 43, Table A3.2. [b] This value at 293 K from ref 44 was obtained from measurements of the viscomagnetic effect; 40 ± 3 Å² at 224 K and 67 ± 5 Å² at 154 K were also reported. [c] This value was obtained from heat conductivity in a magnetic field at room temperature.[45] [d] This is calculated from relaxation measurements in CD_4 gas,[46] and $eqQ/\hbar$ from molecular beam spectroscopy.[47] [e] $\sigma(0001)$ at 309.5 K is 5.15 Å² from ref 48. This value, 5.4 Å² at 300 K, is extrapolated from their table of values for 309.5–425.65 K. [f] Ultrasonic experiments on volume viscosity give $\sigma(0001)$. This experimental value is at 293 K; other values are 15.5, 8.9, and 6.2 Å² at 77.1, 180, and 260 K.[49] [g] See text. [h] This is a gas kinetic viscosity cross section value at 293 K from ref 51. Cross sections 47.1 ± 0.5 and 55.1 ± 0.6 Å² respectively at 224 and 154 K were also reported. [i] This unified set of effective cross sections for $^{12}CH_4$ at 309.5 K are based entirely on experiment and have been derived from the thermal conductivity in the limit of zero density and the first density coefficient of thermal conductivity by Millat and co-workers.[48]

The cross sections for the collisions of CH_4 with CH_4, N_2, Ar, CO_2, and CF_4, obtained independently by us from ^{13}C and ^1H T_1 measurements in physically different gas samples agree within experimental errors. In each of the these five collision pairs the temperature dependence of the ^{13}C data is somewhat steeper than the ^1H data and slightly more pronounced for CF_4 and Ar collision partners. This could be a real difference, which could be attributed to small non-spin–rotation (non-SR) contributions to ^1H relaxation rates. However, the data are not good enough to say definitively that there are significant non-SR contributions to ^1H relaxation in these samples at these temperatures. In any case, Table I had shown no temperature dependence in the ratio $T_1(^1H)/T_1(^{13}C)$, which would indicate that there are no significant non-SR contributions to ^1H relaxation due to CH_4–CH_4 collisions at these temperatures.

The cross sections for rotational angular momentum transfer at 300 K have been calculated from the proton relaxation times from other laboratories and are compared with cross sections obtained from our ^1H and ^{13}C measurements. For the collisions of CH_4 with CH_4, N_2, Ar, and CO_2, Table IV shows that all cross sections at room temperature agree within experimental errors.

However, the literature values for the temperature dependence of CH_4–N_2 and CH_4–CO_2 do not agree with ours.

Discussion

Effective cross sections for CH_4–CH_4 collisions that cause changes in the **J** vector, σ_J (represented by the symbol $\sigma'(0\hat{1})$ in the notation of Beenakker et al.[42]) may be compared with various effective cross sections obtained from other observables. These are shown in Table V, where $\sigma(20)$ is the gas kinetic viscosity cross section and $\sigma(02\pi)$ the reorientation cross section for the **JJ'** tensor, $\sigma(0001)$ is the cross section for transfer of internal energy to translational energy, and $\sigma'(0\hat{2})$ or σ_θ and $\sigma'(0\hat{1})$ (or σ_J) are respectively the cross sections associated with the quadrupolar and spin rotation relaxation in CD_4 and CH_4. The cross sections associated with thermal conductivity, $\sigma(10E)$ and $\sigma(10D)$, are defined in ref 56, where the general form of the notation used in Table V is explained.

σ_{rot}(IRDR) is a cross section obtained from an infrared double-resonance laser spectroscopic technique, which measures the total rate of depopulation of specific rotational states by collisions and also the rates of transfer into specific final rovibrational states. This value, 41.9 ± 0.8 Å^2, is for the ground vibrational state of $^{13}CD_4$ molecule.[52] A larger cross section was obtained for a vibrationally excited state of the molecule.

The different averaging (over the rotational states) associated with IRDR compared to other measurements of rotational relaxation in methane, such as the $\sigma_{rot}(0001)$ from sound absorption data, have been discussed by Foy et al.[52] The rotational contribution $\sigma_{rot}(0001)$ = 6.5 Å^2 was derived from the full cross section $\sigma(0001)$ by using the heat capacities for internal rotational and vibrational motion, and also $\sigma_{vib}(0001)$ from vibrational collision numbers in the literature, in the equation

$$c_{int}\sigma(0001) = c_{rot}\sigma_{rot}(0001) + c_{vib}\sigma_{vib}(0001)$$

For details see ref 50, where values for other temperatures (180, 260, and 293 K) are also given. $\sigma_{rot}(0001)$ is a cross section for the rotationl-to-translational energy transfer, whereas $\sigma(0001)$ is for the energy transfer from all internal degrees of freedom to translational. The independently obtained value of $\sigma_{rot}(0001)$ for CD_4 is larger than that for CH_4 by a factor $(m_{CD_4}/m_{CH_4})^{1/2}$ = 1.12.[49]

TABLE VI: Comparison of Efficiency of Collisions in Causing Changes in the Rotational Angular Momentum Vector in CH_4 and CO_2

$(\sigma_J/\sigma_{geom})_{CH_4}$ [a]		$(\sigma_J/\sigma_{geom})_{CO_2}$ [b]	
CH_4–CH_4	0.42	0.64[c]	CO_2–CH_4
CH_4–N_2	0.39	0.62	CO_2–N_2
CH_4–CO	0.38		CO_2–CO
CH_4–Ar	0.39	0.83	CO_2–Ar
CH_4–HCl	0.60	1.35	CO_2–HCl
CH_4–CO_2	0.55	1.34	CO_2–CO_2
CH_4–CF_4	0.44	1.12[c]	CO_2–CF_4
CH_4–Kr	0.43	1.2	CO_2–Kr
CH_4–Xe	0.49	1.4	CO_2–Xe
CH_4–SF_6	0.53	1.5	CO_2–SF_6

[a] $\sigma_{geom} = \pi r_0^2$, where r_0 is taken from ref 43, Table A3.2, except for CH_4–CO and CH_4–HCl, which were obtained as arithmetic means of the r_0 for like pairs, r_0(CO–CO) = 3.592 Å,[61] r_0(HCl–HCl) = 3.339 Å.[62] [b] Reference 23. [c] Reference 66.

The pressure broadening cross sections from IR and Raman spectra are different from each other. Gordon's semiclassical theory[53] provides the definitions of these cross sections as follows:

$$\sigma_{PB}(\text{IR}) = (1/\bar{v})\left(v\int_0^\infty [1 - P_{el}\cos\eta\cos^2(\tfrac{1}{2}\alpha)]2\pi b\,db\right)$$

$$\sigma_{PB}(\text{Raman}, Q) = (1/\bar{v})\left(v\int_0^\infty [1 - P_{el}\exp(-i\eta_{vib})(\tfrac{3}{2}\cos^2\alpha - \tfrac{1}{2})]2\pi b\,db\right)$$

where P_{el} is the probability that the J quantum number is not changed by the collision. Collisions that change m_J (reorienting collisions) are included in P_{el}. η and η_{vib} are the rotational and vibrational phase shifts, and α is the angle through which the angular momentum vector is reoriented by the collision. These cross sections are usually J dependent. The typical value σ_{PB}(IR) = 69 Å^2 is calculated from the self-broadening coefficients of the $^{12}CH_4$ $R(0)$ line in the ν_4 R branch at 296 K, measured by Ballard and Johnston.[54] There is a tetrahedral symmetry dependence, i.e., pressure-broadening coefficients are different from A, E, and F transitions, leading to $\sigma_{PB}(F) > \sigma_{PB}(A) > \sigma_{PB}(E)$.[54,57] Pressure broadening by other collision partners such as N_2, H_2, and He have been reported as well.[57] The cross section σ_{PB}(Raman, Q) = 82 Å^2 is calculated from the collisional broadening coefficient γ = 0.0843 cm^{-1} atm^{-1} obtained by least-squares Voigt profile fit to experimental stimulated Raman spectra $Q(3)$ and $Q(4)$ lines of $^{13}CD_4$ at 295 K in the pentad region of the spectrum.[55] The difference between the cross sections from pressure-broadening and IRDR measurements have been discussed by Foy et al.[52b]

The relative magnitudes of the different cross sections

$$\sigma_{PB} > \sigma(12q) > \sigma_\theta > \sigma(20) > \sigma(10D) > \sigma(02\pi) > \sigma(10E) > \sigma_J > \sigma(0001)$$

is in the same rank order as for CO–CO[23,56] but not the same as for CO_2–CO_2.[23,56,58] Each of the cross sections in Table V has a well-defined and unique dependence on the nonspherical part of the intermolecular potential function. McCourt and co-workers have shown that these effective cross sections can be calculated from an available potential surface by scattering calculations, full classical trajectory, or the cheaper infinite-order sudden approximation (IOS) calculations, such as have been reported for the N_2–Ne pair.[59] When compared with the experimentally derived values in Table V, the anisotropy of proposed potential surfaces for CH_4–CH_4 can be tested. Of course, only full quantum scattering calculations such as those by Smith and Secrest[60] on CH_4–Ar could expect to reproduce the T_d symmetry dependence

(42) Beenakker, J. J. M.; Knaap, H. F. P.; Sanctuary, B. C. In *Transport Phenomena*; AIP Conference Proceedings, 1973; pp 21–49.
(43) Maitland, G. C.; Rigby, M.; Smith, E. B.; Wakeham, W. A. *Intermolecular Forces, Their Origin and Determination*; Clarendon Press: Oxford, 1981.
(44) Urbaniak, J. L.; Reesor, G. E.; Dagg, I. R. *Can. J. Phys.* **1976**, *54*, 1606–1612.
(45) Hermans, L. J. F.; Koks, J. M.; Hengeveld, A. F.; Knaap, H. F. P. *Physica* **1970**, *50*, 410–432.
(46) Beckmann, P. A.; Bloom, M.; Burnell, E. E. *J. Chem. Phys.* **1986**, *84*, 5898–5905.
(47) Wofsy, S. C.; Muenter, J. S.; Klemperer, W. *J. Chem. Phys.* **1970**, *53*, 4005–4014.
(48) Millat, J.; Ross, M.; Wakeham, W. A.; Zalaf, M. *Physica A* **1988**, *148*, 124–152.
(49) Prangsma, G. J.; Alberga, A. H.; Beenakker, J. J. M. *Physica* **1973**, *64*, 278–288.
(50) Millat, J.; Plantikow, A.; Mathes, D.; Nimz, H. *Z. Phys. Chem. (Leipzig)* **1988**, *269*, 865–878.
(51) Burgmans, A. L. J.; van Ditzhuyzen, P. G.; Knaap, H. F. P.; Beenakker, J. J. M. *Z. Naturforsch. A* **1973**, *28*, 835–848.
(52) (a) Foy, B.; Laux, L.; Kable, S.; Steinfeld, J. I. *Chem. Phys. Lett.* **1985**, *118*, 464–467. (b) Foy, B.; Hetzler, J.; Millot, G.; Steinfeld, J. I. *J. Chem. Phys.* **1988**, *88*, 6838–6852.
(53) Gordon, R. G. *J. Chem. Phys.* **1966**, *44*, 3083–3089.
(54) Ballard, J.; Johnston, W. B. *J. Quant. Spectrosc. Radiat. Transfer* **1986**, *36*, 365–371.
(55) Millot, G.; Lavorel, B.; Chaux, R.; Saint-Luop, R.; Pierre, G.; Berger, H.; Steinfeld, J. I.; Foy, B. *J. Mol. Spectrosc.* **1988**, *127*, 156–177.
(56) Van Houten, H.; Hermans, L. J. F.; Beenakker, J. J. M. *Physica A* **1985**, *131*, 64–103.
(57) Fox, K. *J. Chem. Phys.* **1984**, *80*, 1367–8.
(58) Millat, J.; Mustafa, M.; Ross, M.; Wakeham, W. A.; Zalaf, M. *Physica A* **1987**, *145*, 461–497.
(59) Wong, C. C. K.; McCourt, F. R. W.; Dickinson, A. S. *Mol. Phys.* **1989**, *66*, 1235–1260.
(60) Smith, L. N.; Secrest, D. *J. Chem. Phys.* **1981**, *74*, 3882–3897.

of the pressure-broadening cross sections.[57]

The ratios of the spin relaxation cross sections to the geometric cross sections are shown in Table VI. These ratios are small compared to those obtained for CO_2. It takes two or three "hard-sphere" collisions to cause a change in rotational angular momentum of the CH_4 molecule. Since the first nonvanishing electrical moment in CH_4 is the octopole moment, the long-range anisotropy of CH_4 is weaker than that of CO_2, making CH_4 a less effective collision partner. The efficiencies of CH_4-X collisions increase with increasing polarizability of X, except for the enhanced efficiency of CH_4-CH_4 collisions, which may be attributed to the matching of rotational energy levels which increase the likelihood of rotational energy exchange.

Empirical potentials for CH_4-N_2 and CH_4-CO_2 and CH_4-He, Ne, Ar have been derived from ^1H relaxation times by Lalita et al.[38-40] using the Bloom-Oppenheim theory of spin relaxation, with additional assumptions.[63] The correlation time of the spin rotation interaction for a given J state is assumed to be equal to the average lifetime of the molecule in that J state, the latter being calculated from transition rates obtained by using the "constant acceleration" approximation. Three parameters in the anisotropy were obtained while using effective ϵ and r_0 from viscosity data in the isotropic potential. Our results lead us to question the reliability of their empirical potentials. It appears that their procedure is feasible only if the temperature dependence of T_1 differs markedly from $T^{-3/2}$. We find, however, that for CH_4-X the deviations from $T^{-3/2}$ dependence are relatively small, smaller than those observed by us in CO_2-X or N_2-X for almost all X.[23,64] Furthermore, the comparison of the temperature dependence reported for CH_4-N_2 and CH_4-CO_2 by Lalita et al. with ours in Table IV indicates that there may have been some systematic errors in their measurements or data analysis. Their method of extrapolating to a composition that is 100% in the buffer gas could give rise to larger errors in the temperature dependence of the probe-buffer relaxation times.

The ratio of the two cross sections obtained from NMR relaxation times, $\sigma_\theta/\sigma_J = 2.9$ means that $\tau_\theta = \tau_J/2.9$ in the gas phase at 300 K. This can be compared with a limiting case of an extended diffusion model of fluids. Gordon's model, which assumes that collisions change the angular momentum of the molecules and that the molecules rotate freely between collisions, has been applied to spherical top molecules.[65] In this model τ_J is the mean time between collisions that either randomize both the magnitude and the orientation of the angular momentum of the molecule (J diffusion) or only its orientation (M diffusion). For diffusion in the weak friction limit (low gas densities), McClung finds $\tau_\theta = \tau_J/4$,[65] in reasonably good agreement with our $\tau_\theta = \tau_J/2.9$ for CH_4 gas.

Conclusions

We have established that spin-rotation dominates both ^1H and ^{13}C relaxation in CH_4 in the gas phase. Therefore we can express our experimental results in terms of a single temperature-dependent cross section $\sigma_J(T)$. This cross section is well-defined according to Gordon's theory in terms of the scattering matrix elements for calculations on a trial potential energy surface. These $\sigma_J(T)$ can be used together with other experimental data such as virial coefficients,[15] diffusion coefficients,[14] total differential scattering cross sections,[11-13] collision-induced microwave absorption,[44] collision-induced rotational Raman scattering,[2] and the various cross sections given in Table V, to fit a CH_4-CH_4 or CH_4-X potential surface.

Acknowledgment. This research was supported in part by the National Science Foundation (Grants CHE85-05725 and CHE89-01426).

(61) Trengove, R. D.; Robjohns, J. L.; Dunlop, P. J. *Ber. Bunsen-Ges. Phys. Chem.* **1984**, *88*, 450-453.
(62) Turfa, A. F.; Marcus, R. A. *J. Chem. Phys.* **1979**, *70*, 3035-3040.
(63) Bloom, M.; Oppenheim, I. *Adv. Chem. Phys.* **1967**, *12*, 549-599.
(64) Jameson, C. J.; Jameson, A. K.; Smith, N. *J. Chem. Phys.* **1987**, *86*, 6833-6838.
(65) McClung, R. E. D. *J. Chem. Phys.* **1969**, *51*, 3842-3852.
(66) Jameson, C. J.; Jameson, A. K. *J. Chem. Phys.* **1990**, *93*, 3237-3244.

Preparation of Copper-Poly(2-vinylpyridine) Nanocomposites†

A. M. Lyons,*,‡ S. Nakahara,‡ M. A. Marcus,‡ E. M. Pearce,§ and J. V. Waszczak‡

AT&T Bell Laboratories, Murray Hill, New Jersey 07974, and Polytechnic University, Brooklyn, New York 11201 *(Received: October 9, 1989; In Final Form: August 21, 1990)*

Ultrafine copper particles were prepared in a poly(2-vinylpyridine) matrix by the thermal decomposition of a copper formate-poly(2-vinylpyridine) complex. The steric bulk of the polymeric ligand precludes complexation of more than one pyridine moiety around copper and ensures solubility of the complex. At temperatures above 125 °C, a redox reaction occurs where Cu^{2+} is reduced to copper metal and formate is oxidized to CO_2 and H_2. The decomposition reaction was studied by thermogravimetric analysis, differential scanning calorimetry, and mass spectrometry. Copper concentrations up to 23 wt % have been incorporated into the polymer by this technique. The presence of the polymeric ligand induces the redox reaction to occur at a temperature 80 °C lower than in uncomplexed copper formate. Incorporation of the reducing agent (formate anion) into the polymer precursor enables the redox reaction to occur in the solid state. Films of the polymer precursor were prepared, and the formation of metallic copper particles was studied by visible and infrared spectroscopy, X-ray diffraction techniques, transmission electron microscopy, and extended X-ray absorption fine structure (EXAFS). Results from these measurements indicate that spherical copper particles with an average diameter of 35 Å are isolated within the polymer matrix. The particles are thermodynamically stable at temperatures up to the decomposition of the polymer matrix (≈350 °C) but oxidize rapidly upon exposure air.

Introduction

Nanocrystalline composites are composed of ultrafine particles, with diameters ranging from 1 to 20 nm, dispersed in a matrix. These materials exhibit unique properties, different from normal crystalline or glassy materials,[1,2] which can be attributed to the enormous surface area of the ultrafine particles. A metal particle several nanometers in diameter has roughly half of its constituent

† Taken from the dissertation of A. M. Lyons submitted to the Faculty of the Polytechnic University in partial fulfillment of the requirements for the degree Doctor of Philosophy (Chemistry), June 1, 1987.
‡ AT&T Bell Laboratories.
§ Polytechnic University.

(1) Andres, R. P.; et al. *J. Mater. Res.* **1988**, *4*, 704.
(2) Birringer, R.; Herr, U.; Gleiter, H. *Proc. JIMIS 4 (1986), Suppl. Trans. Jpn. Inst. Met.* **1986**, *27*, 43.

0022-3654/91/2095-1098$02.50/0